The Galactic Bulge

Ken C. Freeman

Abstract I will give a brief overview of galactic bulges and then discuss in more detail what is known about the bulge of our Galaxy. The Milky Way has a small boxy/peanut-shaped bulge which we believe formed via instabilities of the disk rather than through mergers. The bulge of the Milky Way therefore appears to be a dynamical product of the early Galactic disk, without significant contamination from mergers with other galaxies. The instabilities are believed to have occurred about 2 Gyr after the inner stellar disk was formed. The bulge therefore contains a relatively clean sample of the early disk as it was about 8 Gyr ago, trapped dynamically within the boxy bulge structure. The various components of the early disk (young thin disk, older thin disk, thick disk) are visible as substructure in the stellar metallicity distribution function and kinematics of the bulge stars.

1 Introduction

Galactic bulges are not an essential part of the formation process of disk galaxies, but when they do occur they can give some useful insights into the early evolution of their parent galaxies. The size of galactic bulges varies greatly from galaxy to galaxy, from vanishingly small to much more luminous than the disks of their parent galaxy (as in the Sombrero galaxy NGC 4594). Galaxies with relatively large circular velocities can have small bulges, as in the Milky Way. Such galaxies are not rare. Kormendy et al. (2010) found that giant galaxies with small bulges are common in the local neighborhood.

Large bulges are predominantly more or less round, while the smaller bulges often have a distinct boxy or peanut shape. The current belief is that large bulges are associated with merger events (e.g. Toomre 1977; Abadi et al. 2003). The smaller boxy bulges (like the bulge of the Milky Way) are believed to arise from instabilities of rotating stellar disks and are probably unrelated to merger events (e.g. Combes and Sanders 1981). The next section is on a large galaxy NGC 1316 which has had

K. C. Freeman (✉)
Research School of Astronomy & Astrophysics, Mount Stromlo Observatory,
The Australian National University, Canberra, Australia
e-mail: kcf@mso.anu.edu.au

K. Freeman et al. (eds.), *Lessons from the Local Group,*
DOI 10.1007/978-3-319-10614-4_3

Fig. 1 The late merger galaxy NGC 1316 in the Fornax cluster (Martin Pugh: APOD 2008)

a relatively recent major merger and appears now to be in the process of evolving towards a system like the Sombrero galaxy. Later sections focus on the bulges of later-type galaxies, including the Milky Way.

2 The Late-Merger System NGC 1316

NGC 1316 is a bright late-merger galaxy in the Fornax cluster which seems destined to evolve into a Sombrero-like disk galaxy with a large bulge. It is very bright ($M_B = -22.5$) with a Sersic index of about 6, appropriate to a large bulge or elliptical galaxy. Its light distribution still shows prominent structure in its outer regions (see Fig. 1), characteristic of a late-merger remnant. The color distribution of its globular clusters show that its youngest clusters have ages of about 3 Gyr (Goudfrooij et al. 2001), so this is the likely epoch of its last major merger-driven star formation event.

McNeil-Moylan et al. (2012) measured velocities of 796 planetary nebulae in NGC 1316, using counter-dispersed spectroscopy with the FORS2 spectrograph on the VLT. The optical light of late-type galaxies like NGC 1316 is dominated by low-mass giant stars. Planetary nebulae (PN) are the late stages of evolution of stars with masses less than about 8 $M_\odot$, so they are good tracers of the starlight. During the brief planetary nebula phase, about 15 % of the energy of the central star is converted into a single line of [OIII], which makes it possible to detect PN in the outer parts of galaxies at distances of many Mpc and measure their velocities (See the paper by Arnaboldi in this volume for more details about using PN as dynamical tracers in distant galaxies).

With such a large sample of tracer objects, it is possible to measure the rotational velocity and velocity dispersion of NGC 1316 out to a radius of about 50 kpc. The velocity dispersion σ drops from about 250 km s^{-1} at the center to about 130 km s^{-1} at 50 kpc, while the rotational velocity of the planetary nebulae is roughly constant at about 100 km s^{-1} from 10 kpc to 50 kpc (see Fig. 2). Much of the angular

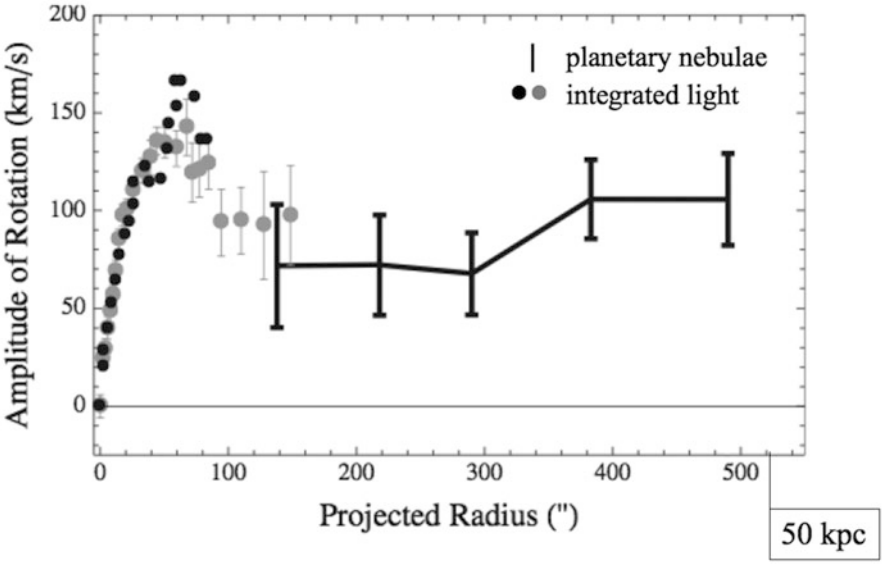

Fig. 2 The rotation curve of the starlight and the planetary nebulae in NGC 1316 (from McNeil-Moylan et al. 2012)

momentum of this merger remnant resides in its outer regions. McNeil-Moylan et al. (2012) successfully modelled the kinematics of the planetary nebulae with a Jeans model of constant anisotropy (β-parameter $= 0.5$) and a stellar mass-to-light ratio $M/L_B = 2.8$. In addition to the stellar component, a massive dark halo with a velocity dispersion of 289 km s^{-1} is needed to model the kinematics over the whole range of radius out to 50 kpc. This dark halo contributes about 80% of the total mass within 50 kpc. In summary, this post-merger galaxy appears to be approaching equilibrium: its dark halo is in place and the outer parts of its stellar component contain a substantial amount of ordered angular momentum. NGC 1316 is a relatively dusty system, so is likely to contain a significant amount of residual gas. Neutral hydrogen observations are difficult because NGC 1316 (Fornax A) is one of the brightest radio continuum sources in the sky (see Horellou et al. 2001 for a summary of its atomic and molecular gas content).

We can compare NGC 1316 with the more settled Sombrero galaxy which has a very large bulge and a rapidly rotating disk. Its bulge has a velocity dispersion of about 200 km s^{-1} (Kormendy and Illingworth 1982) and its stellar disk is rotating at about 300 km s^{-1} (Wagner et al. 1989). The rotation seen in HI is even larger: about 350 km s^{-1} (Bajaja et al. 1984). It seems likely that NGC 1316 will evolve into a system comparable to the Sombrero galaxy: from its velocity dispersion and integrated magnitude, its bulge may be even larger than the Sombrero's. The circular velocity of its dark halo as derived by McNeil-Moylan et al. indicates that the final disk of the evolved NGC 1316 will have a large circular velocity, rather similar to that of the Sombrero system.

3 The Bulges of Later-Type Galaxies

Later-type galaxies like the Milky Way mostly have small boxy bulges with near-exponential light distributions (e.g. Courteau et al. 1996). These small bulges are probably not merger products but were more likely generated by instabilities of the disk itself. The association of boxy bulges with the bar-forming and bar-buckling instabilities of disks goes back at least to the simulations by Combes and Sanders (1981) and the observations of Kuijken and Merrifield (1995) and Bureau and Freeman (1999). The observational association is based on long-slit spectra of edge-on disk galaxies with boxy bulges which show complex gas flows in their inner regions driven by the asymmetric rotating bar-like potential of the boxy bulge.

These flows are seen in all boxy bulge galaxies with gas in their inner regions: NGC 5746 is a particularly nice example (Bureau and Freeman 1999). The stellar kinematics of boxy bulges show a characteristic cylindrical rotation: the mean rotational velocity of the stars in the bulge depends mainly on the radius and only very weakly on the height above the plane. This was seen observationally by Kormendy and Illingworth (1982) and appears also in the simulations of boxy bulges that arise from disk instabilities.

4 The Galactic Bulge

Several recent surveys of stars in the Galactic bulge have studied its kinematics and chemical properties. Here I will discuss mainly the recent large ARGOS stellar survey of the bulge (Ness et al. 2012, 2013a, b; Freeman et al. 2013). The ARGOS survey acquired spectra of 28,000 candidate red giants towards the bulge and inner disk, with a spectral resolving power of about 11,000. This provides accurate radial velocities and the resolution is sufficient to measure abundances of Fe and most of the $\alpha-$elements.

The goal of the survey was to explore the idea that the Galactic bulge grew from the disk via bar-buckling instabilities. Rotating disks are often unstable to forming a flat bar structure at their centers. The bars grow naturally from instabilities of a disk that is dynamically relatively cold. The flat bar is in turn often unstable to vertical buckling which generates the boxy appearance of the bar seen edge-on. In the bar-buckling scenario, the bulge *structure* is younger than its oldest stars, which were originally part of the disk. In the N-body simulations, it typically takes about 2 Gyr for the bar to form in the disk and then to buckle vertically to generate the peanut-shaped bulge. So the stars of the bar/bulge may be chemically similar to stars of the adjacent thin and thick disk that are about 8 Gyr old.

The 28 fields of the ARGOS survey are shown in Fig. 3. They cover the southern bulge at latitudes $b = -5°, -7.5°$ and $-10°$, plus three relatively transparent northern bulge fields and some fields extending out into the adjacent thin and thick disk. The lines of sight through these fields pass through most of the Galactic components. The thin disk, the thick disk, the bulge itself, the stellar halo and the young spiral

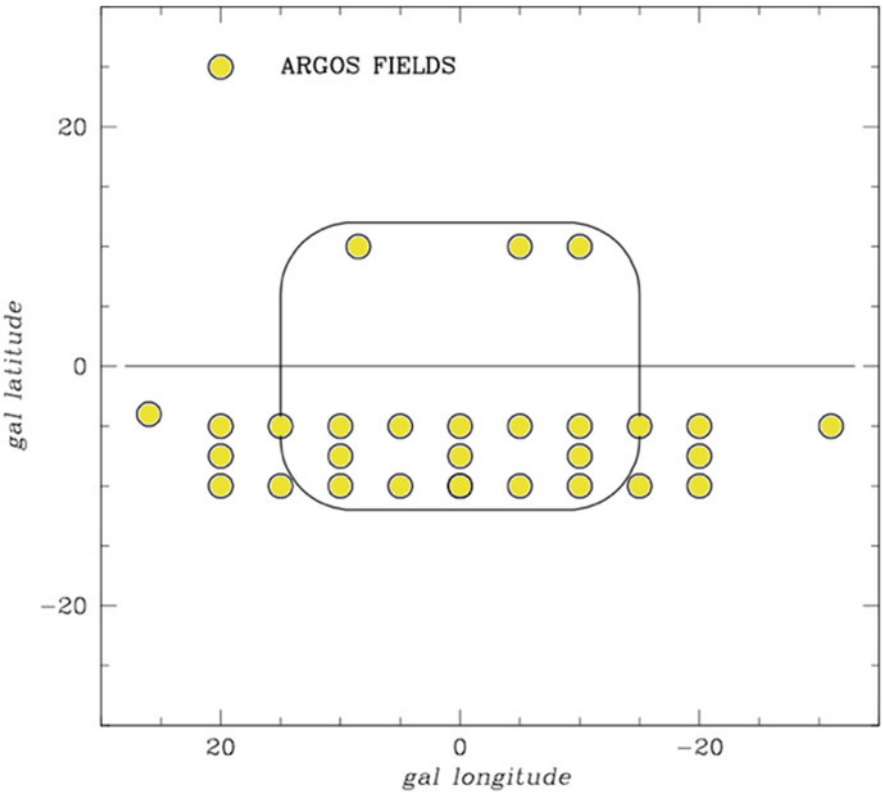

Fig. 3 The location of the ARGOS survey fields in galactic latitude and longitude. The filled circles show the 28 fields, each of about 1000 stars, and the rounded rectangle indicates the outline of the outer bulge

arm populations will all be represented along the line of sight. Because the bulge is at the center of the Galaxy, we expect to see the denser central regions of all of these Galactic components.

In order to study the stars of the bar/bulge, we need to reduce contamination by stars that lie in front of and behind the bulge, so photometric or spectroscopic parallaxes are needed. Ideally we would use stars for which relatively accurate distances can be derived. At a distance of about 8 kpc, large samples of spectra are possible only for the red giant stars. The Galactic bar/bulge is currently believed to lie at an angle of about 25° to the sun-center line and extends about 3 kpc from the center towards and away from us. The ARGOS stars were therefore selected from the 2MASS point source catalog, to have colors and magnitudes appropriate to giants within the bar region. Because metal-poor stars in the bulge region are interesting, as members of the inner stellar halo and also as potential first stars (eg Tumlinson 2010), the color criteria were chosen carefully so that metal-poor stars were not excluded by the selection process. Not all of these stars will turn out to be within the bar/bulge. Distances

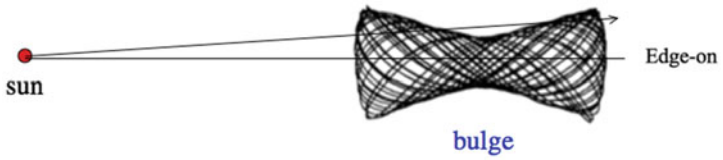

Fig. 4 Lines of sight from the sun through a peanut-shaped bulge seen close to end on. The peanut-shaped object shown here is an example of the kind of stellar orbits (seen edge-on) which support the peanut-shaped bulge. The upper line of sight passes through the two humps of the peanut, so the number of stars per unit length shows two peaks as it passes through the two humps

for the brighter red giants are difficult to measure accurately, but the clump giants have a narrow range of absolute magnitude around a mean $M_K = -1.61$ (Alves 2000) with a dispersion of only about 0.22 about the mean. For the ARGOS stars, we estimated isochrone distances from our temperatures and spectroscopic gravities and metallicities, and then selected stars that lie within a Galactocentric radius $R_G = 3.5$ kpc to be bulge stars.

The errors in the stellar parameters are estimated from observations of independently measured stars in the field, open and globular clusters and the bulge itself. The mean errors in the radial velocity, effective temperature, [Fe/H], [α/Fe] and log g are 0.9 km s^{-1}, 100K, 0.09, 0.10 and 0.30 respectively. Of our 28,000 stars, about 2500 are foreground dwarfs and 11,500 are giants outside the inner 3.5 kpc which we are taking as our bulge region. We see that only half of the stars towards the bulge with giant-like colors are actually giants within the bulge region. Foreground and background contamination is very significant in any such sample.

We were interested to know which stars contribute to the boxy peanut structure of the bulge. Nataf et al. (2010) and MacWilliam and Zoccali (2010) had discovered the bimodal luminosity function of clump giants along particular lines of sight through the bulge. The bimodality is interpreted as arising from the distribution of stars along the line of sight as it passes through the two humps of the peanut (see Fig. 4). The same bimodality is seen in the ARGOS sample, but only for the stars that are more metal-rich than [Fe/H] $= -0.5$. The more metal-poor stars are not part of the peanut structure. In the next section, we will discuss the likely reason.

5 The Metallicity Distribution of Bulge Stars

The metallicity distribution function (MDF) of the large sample of ARGOS bulge stars is broad, extending over the range [Fe/H] $= -1.0$ to $+0.5$ with a sparse tail of stars down to [Fe/H] < -2. The sample is large enough for structure in the MDF to be visible. All of the ARGOS fields show the same component structure as seen in Fig. 5. The Bayesian information criterion gives the optimal number of components for the MDF to be between 4 and 5. The main body of bulge stars with [Fe/H] between -1.0 and $+0.5$ has 3 distinct metallicity components denoted A, B and C

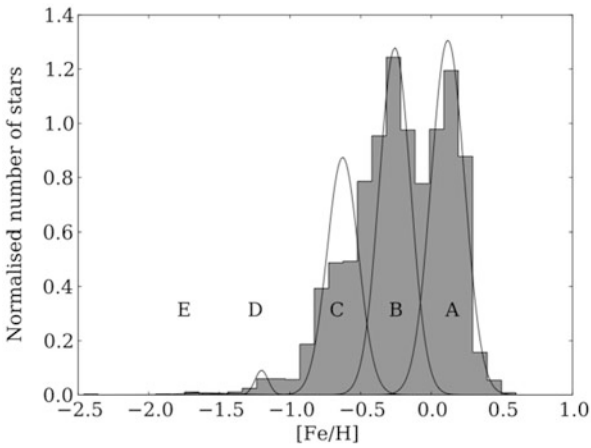

Fig. 5 The metallicity distribution of stars at $b = -5°$ in the bulge shows three major components denoted A, B and C, plus two weak metal poor components D and E. The relative weights of components A–C change with galactic latitude. The most metal rich component A is strong at lower latitudes but decreases in importance at higher latitudes (from Ness et al. 2013a)

as seen in Fig. 5, and their relative weights change with position in the bulge. The metal-richest component A is strongest near the Galactic plane, and the more metal-poor component C is stronger at higher latitudes. This changing weight generates an apparent vertical metallicity gradient in the bulge. Only components A and B are involved in the peanut structure of the bulge.

The MDF for stars in the inner disk field at $l = -31°, b = -5°$ show all of the same metallicity components that are seen within the bulge, with weights similar to those in the bulge at $b = -5°$. In the inner disk, these components are probably present in their undisturbed form, as disk stars, while in the bulge the stars of these components have been trapped dynamically into the bulge via the bar-forming and bar-buckling instability. Component A is weakly $\alpha-$enhanced (Fig. 6) and is strongly involved in the peanut bulge structure. We tentatively interpret component A as the colder more metal-rich part of the early thin disk. Component B is $\alpha-$enhanced

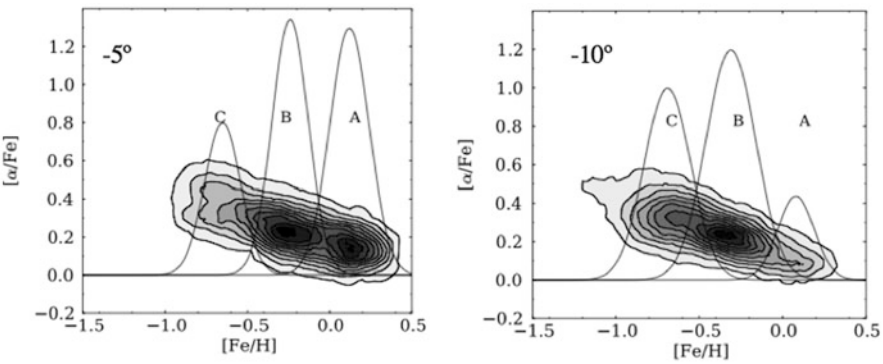

Fig. 6 The [α/Fe] - [Fe/H]) distribution of the bulge stars at $b = -5°$ and $-10°$ (from Ness et al. 2013a)

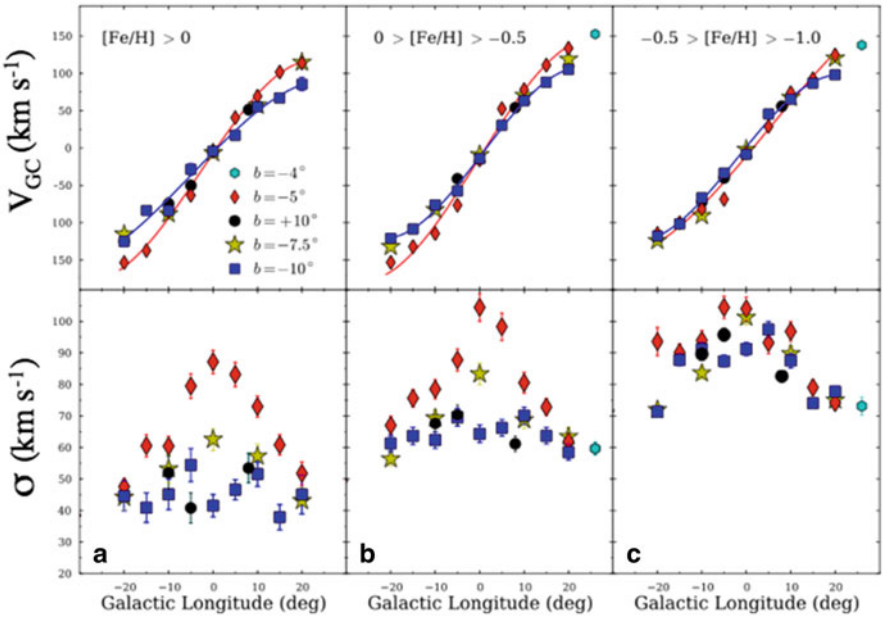

Fig. 7 The upper panels show the Galactocentric cylindrical rotation of the three major components of the Galactic bulge, corrected for the standard solar motion and an LSR circular velocity of 220 km s^{-1}. The different galactic latitude samples are shown by different symbols. The lower panels show their line of sight velocity dispersions. The shape of the velocity dispersion distributions is similar for components A and B, but the velocity dispersion of the metal-rich component A is clearly smaller (from Ness et al. 2013b)

and is the main component of the peanut bulge structure. Component C is more metal-poor and more $\alpha-$enhanced but not part of the bulge's peanut structure. Its stars have a similar range of [Fe/H] and [α/Fe] to the thick disk stars near the sun, so component C may be the stars of the early inner thick disk, now locked in the bulge, that were dynamically too hot to become significantly involved in the vertical redistribution of stars that lead to the peanut structure.

6 Kinematics of the Bulge Components

The mean rotation of the stars in the Galactic bulge ($-10^\circ < l < 10^\circ$) is close to cylindrical, as expected for a boxy bulge and found earlier by Kunder et al. (2012) from the BRAVA survey of cooler bulge giants (see Fig. 7). At larger $|l|$, extending out into the surrounding disk, the mean stellar rotation continues to increase up to more than 150 km s^{-1} in the disk at $|l| = 20^\circ$.

Component B rotates more rapidly than component A over the region of the bulge and is dynamically hotter (Ness et al. 2013b). As they are both moving in the same

potential gradient, this suggests that component A is more radially concentrated than component B. We have already seen from Fig. 5 that component A is the most vertically concentrated of the three major bulge components.

The two metal poor components D and E have very different kinematics. Their rotation is much smaller and the velocity dispersion higher, consistent with being part of the inner metal-poor halo of the Galaxy.

7 Interpretation of the Bulge Components

In the instability scenario for formation of the Galactic bulge, the disk evolved chemically and dynamically for about 2 Gyr before becoming unstable and buckling into the peanut structure. We can regard components A–E as relics of the early Galactic disk and halo which were trapped into the bulge by the action of the instability.

The instability process generates a mapping of the stars of the early disk into the boxy/peanut structure. In this way, the bulge preserves a dynamical imprint of the chemical distribution of the disk at the time that the buckling occurred. The bulge gives a chemical snapshot of the MDF of the early disk captured in the bar.

The mapping of disk into bulge depends on the location and motions of the stars at the time of the instability. Kinematically colder stars can suffer strong radial and vertical migration, and can therefore be strongly involved in the peanut structure (components A and B). Di Matteo et al. (2014) studied the N-body mapping of the early disk into the boxy bulge during the epoch of bar formation and buckling (see also Martinez-Valpuesta and Gerhard 2013). In their model, the bar begins to grow after about 0.8 Gyr, the vertical instability starts at 2 Gyr and the system is close to equilibrium by 4 Gyr. During the period of bar formation, the asymmetric gravitational field is changing rapidly, the Jacobi integrals of the stars are not conserved and substantial radial migration of disk stars occurs. This may be the event that brought the metal-rich stars from the inner Galaxy into the solar neighborhood (see e.g. Haywood 2008).

The instability maps stars from the entire disk into the bulge. Stars from the inner (outer) disk are preferentially mapped into the inner (outer) regions of the bulge. The boxy structure is defined by stars that initially have orbital radii $> 0.7 r_{bar}$ and lie near the vertical inner Lindblad resonance. Stars from the inner region are seen to migrate far out into the disk, and stars from larger radii migrate in to the bar. The N-body models suggest that components A and B originate in the early disk, with the stars of the compact metal-rich component A coming from nearer the center than the stars of the more extended and rapidly rotating component B. Component C, which is not involved in the peanut structure, is believed to come from the (hotter) old thick disk.


-KEN FREEMAN-

Acknowledgements I am grateful to Lia Athanassoula, Ortwin Gerhard, John Kormendy, Inma Martinez-Valpuesta and Melissa Ness for many discussions about bulges. My best wishes to David Block and Bruce Elmegreen on this notable occasion.

References

Abadi, M.G., Navarro, J.F., Steinmetz, M., Eke, V.R. 2003. ApJ, 597, 21
Alves, D. 2000. ApJ, 539, 732.
Bajaja, E., van der Burg, G. et al. 1984. A&A, 141, 309.
Bureau, M. & Freeman, K. 1999. AJ, 118, 126.
Combes, F. & Sanders, R. 1981. A&A, 96, 164.
Courteau, S., de Jong, R. et al. 1996. ApJ, 457, L73.
Di Matteo, P., Haywood, M. et al. 2014. astro-ph/1404.0304.
Freeman, K., Ness, M. et al. 2013. MNRAS, 428, 3660.
Goudfrooij, P., Alonso, M., et al. 2001. MNRAS, 328, 237.
Haywood, M. 2008. MNRAS, 388, 1175.
Horellou, C., Black, J. et al. 2001. A&A, 376, 837
Kormendy, J. & Illingworth, G. 1982. ApJ, 256, 460.
Kormendy, J., Drory, N. et al. 2010. ApJ, 723, 54.
Kunder, A., Koch, A. et al. 2012. AJ, 143, 57.
Kuijken, K. & Merrifield, M. 1995. ApJ, 433, L13.
Martinez-Valpuesta, I. & Gerhard, O. 2013. ApJ, 766, L3.
McNeil-Moylan, E., Freeman, K., et al. 2012. A&A, 539A, 11.
Mcwilliam, A. & Zoccali, M. 2010. ApJ, 724, 1491.
Nataf, D., Udalski, A. et al. 2010. ApJ, 721, L28.
Ness, M.K., Freeman, K.C. et al. 2012. ApJ, 756, 22.
Ness, M.K., Freeman, K.C. et al. 2013a. MNRAS, 430, 836
Ness, M.K., Freeman, K.C. et al. 2013b. MNRAS, 432, 2092.
Toomre, A. 1977. in "Evolution of Galaxies and Stellar Populations", ed. B. Tinsley & R. Larson (New Haven: Yale University Observatory), 401.
Tumlinson, J. 2010. ApJ, 708, 1398.
Wagner, S., Bender, R. et al. 1989. A&A, 215, 243.